


# Non-linear mechanical behavior of amorphous glassy polymers: An experimental review

Peihan Lyu(吕沛函), Zhaoyu Ding(丁肇钰), Jiaxin Hao(郝佳欣), Li Peng(彭莉), Wohua Zhou(周沃华), Xianbo Huang(黄险波), and Xingkun Man(满兴坤)

**Citation:**Chin. Phys. B, 2026, 35 (**7**): 078101. DOI: 10.1088/1674-1056/ae1e66
http://cpb.iphy.ac.cn; http://iopscience.iop.org/cpb

**What follows is a list of articles you may be interested in**

---

## Enhancing the thermoelectric performance through the mutual interaction between conjugated polyelectrolytes and single-walled carbon nanotubes

Shuxun Wan(万树勋), Zhongming Chen(陈忠明), Liping Hao(郝丽苹), Shichao Wang(王世超), Benzhang Li(李本章), Xiao Li(黎潇), Chengjun Pan(潘成军), and Lei Wang(王雷)
Chin. Phys. B, 2022, 31 (**2**): 028104. DOI: 10.1088/1674-1056/ac48f9

## Dependence of mechanical properties on the site occupancy of ternary alloying elements in $\gamma'$-$Ni_3Al$: *Ab initio* description for shear and tensile deformation

Minru Wen(文敏儒), Xing Xie(谢兴), Huafeng Dong(董华锋), Fugen Wu(吴福根), Chong-Yu Wang(王崇愚)
Chin. Phys. B, 2020, 29 (**7**): 078103. DOI: 10.1088/1674-1056/ab8a38

## Moisture-sensitive torsional cotton artificial muscle and textile

Yuanyuan Li(李媛媛), Xueqi Leng(冷雪琪), Jinkun Sun(孙进坤), Xiang Zhou(周湘), Wei Wu(兀伟), Hong Chen(陈洪), Zunfeng Liu(刘遵峰)
Chin. Phys. B, 2020, 29 (**4**): 048103. DOI: 10.1088/1674-1056/ab7745

## Universal properties of relaxation and diffusion in condensed matter

K L Ngai(倪嘉陵)
Chin. Phys. B, 2017, 26 (**1**): 018105. DOI: 10.1088/1674-1056/26/1/018105

## Fabrication and formation mechanism of closed-loop fibers by electrospinning with a tip collector

Xu Yan(闫旭), Miao Yu(于淼), Wen-Peng Han(韩文鹏), Ming-Hao You(犹明浩), Jun-Cheng Zhang(张君诚), Rui-Hua Dong(董瑞华), Hong-Di Zhang(张红娣), Yun-Ze Long(龙云泽)
Chin. Phys. B, 2016, 25 (**7**): 078106. DOI: 10.1088/1674-1056/25/7/078106

---

**TOPICAL REVIEW — Masao Doi: Frontiers in soft matter and polymer physics**

# Non-linear mechanical behavior of amorphous glassy polymers: An experimental review

Peihan Lyu(吕沛函)[1], Zhaoyu Ding(丁肇钰)[1], Jiaxin Hao(郝佳欣)[1], Li Peng(彭莉)[2,3], Wohua Zhou(周沃华)[2], Xianbo Huang(黄险波)[2,3,†], and Xingkun Man(满兴坤)[1,4,‡]

[1] *School of Physics, Beihang University, Beijing* 100191, *China*
[2] *National-Certified Enterprise Technology Center, Kingfa Science and Technology Co., Ltd., Guangzhou* 510663, *China*
[3] *Guangdong Provincial Key Laboratory of Special Engineering Plastics (Enterprise), Guangzhou* 510663, *China*
[4] *Peng Huanwu Collaborative Center for Research and Education, Beihang University, Beijing* 100191, *China*

(Received 10 September 2025; revised manuscript received 25 October 2025; accepted manuscript online 12 November 2025)

This review provides an overview of the non-linear mechanical behavior of amorphous glassy polymers under constant strain rate (CSR) testing. These materials exhibit complex responses to mechanical loading, including yielding, strain softening, and strain hardening, arising from the interplay between their out-of-equilibrium structure and the applied deformation. While many studies have addressed isolated aspects of glassy polymer behavior, a unified examination centered specifically on CSR tests remains limited. We first discuss the fundamental origins of non-linearity, including geometric effects and intrinsic mechanisms. Key features of the mechanical response, such as stress–strain curves, volume changes, molecular mobility, and ductile–brittle behavior, are then described. Finally, the effects of critical experimental variables, including strain rate, temperature, hydrostatic pressure, and thermal history (e.g., aging and annealing), are systematically reviewed. By consolidating findings across diverse studies, this review aims to clarify the characteristic mechanical behavior of amorphous glassy polymers in CSR tests and provide a foundation for future experimental and modeling efforts.

**Keywords:** glassy polymers, constant strain rate test, tensile behavior, yielding

**PACS:** 81.05.Lg, 81.40.Jj, 83.60.Df, 83.60.La

**DOI:** 10.1088/1674-1056/ae1e66 **CSTR:** 32038.14.CPB.ae1e66

## 1. Introduction

Amorphous glassy polymers are widely employed in structural, packaging, and biomedical applications due to their favorable mechanical properties, processability, and versatility. For example, glassy composite membranes[1,2] are employed in oil–gas separation and organic vapor recovery, offering advantages such as process simplification, enhanced safety, environmental compatibility, and extended service life. Thermally induced shape memory polymers[3–7] exploit the distinct mechanical responses above and below the glass transition temperature to enable environmental sensing and intelligent actuation. Glassy gels,[7,8] which combine high strength with high modulus, serve as promising substitutes for soft tissues such as cartilage and menisci; through precise control of their microstructure, they can also be engineered into artificial corneas with excellent gas permeability and optical clarity.[9,10]

Amorphous glassy polymers exhibit complex rheological behavior, including non-linear stress–strain responses,[11,12] transitions between glassy and rubbery states,[13,14] and sensitivity to both temperature and loading history,[15,16] as well as to changes in physical and chemical environments.[17,18] To characterize their mechanical behavior, several experimental techniques are employed to probe their viscoelastic and time-dependent behavior. Creep testing, which applies a constant stress and monitors the resulting strain over time, provides insight into long-term deformation under sustained loads and is particularly relevant for service-life prediction. Stress relaxation testing, by maintaining a constant strain and tracking the decay of stress, reveals information about molecular rearrangements and entanglement relaxation processes. In contrast, constant strain rate (CSR) testing imposes deformation at a fixed rate while recording the evolving stress–strain response. This method offers precise control over deformation kinetics, making it highly effective for examining nonlinear viscoelasticity, brittle–ductile transition, yielding, and strain hardening. Owing to its versatility and sensitivity to rate effects and temperature, CSR testing has become a central tool for understanding the fundamental mechanisms governing the deformation of amorphous polymers.[19,20]

This review focuses on the non-linear mechanical behavior of amorphous glassy polymers subjected to constant strain rate testing. Emphasis is placed on experimentally observed phenomena, including stress–strain characteristics, volumetric

†Corresponding author. E-mail: huangxianbo@kingfa.com.cn
‡Corresponding author. E-mail: manxk@buaa.edu.cn

© 2026 Chinese Physical Society and IOP Publishing Ltd. All rights, including for text and data mining, AI training, and similar technologies, are reserved.

changes, and molecular mobility during deformation. We restrict our discussion to amorphous polymers in the glassy state and exclude rubbery or semicrystalline systems to maintain clarity and specificity. Both intrinsic factors (such as molecular structure and segmental dynamics) and extrinsic conditions (such as temperature, strain rate, pressure, and thermal history) are considered in order to elucidate the full range of mechanical responses.

The review is organized as follows. Section 2 introduces the fundamental origins of non-linear behavior, distinguishing between geometric effects and intrinsic material nonlinearity, and introducing the non-linearity arising from experimental procedures. Section 3 summarizes key experimental findings on the mechanical response of glassy polymers under CSR loading, focusing on the evolution of stress–strain curves, volumetric responses, molecular mobility, and intrinsic ductile–brittle behavior. Section 4 examines how these responses are influenced by strain rate, temperature, hydrostatic pressure, and thermal history (i.e., physical aging, annealing, quenching, and rejuvenation). We end with some conclusions and open problems in Section 5.

## 2. Origins of non-linear behavior

Consider a cylindrical sample of a glassy polymer with an initial length $L_0$ and initial cross-sectional area $S_0$, subjected to a uniaxial tensile force $F$, as shown in Fig. 1(a). The mechanical response of the sample can be described in terms of stress and strain, defined in both engineering and true formulations.[22] The engineering stress is given by $\sigma_{\text{eng}} = F/S_0$, and the engineering strain is $\varepsilon_{\text{eng}} = \Delta L/L_0$, with $\Delta L$ representing the change in length. In contrast, the true stress accounts for the instantaneous cross-sectional area and is defined as $\sigma = F/S$, where $S$ is the current area, while the true strain is expressed as $\varepsilon = \int \mathrm{d}L/L = \ln(L/L_0)$, where $L$ denotes the current length of the specimen.

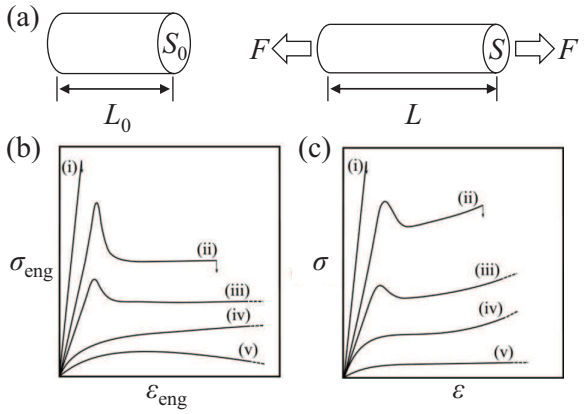



**Fig. 1.** (a) Schematic illustration of the stretching of a cylindrical glassy polymer sample. (b) Typical engineering stress–strain curve and (c) true stress–strain curve of PMMA under uniaxial tension. (i)–(iii) correspond to temperatures around the glass transition temperature, while (iv)–(v) correspond to temperatures above the glass transition temperature, all at identical strain rates. Reproduced from Ref. [21] (CC BY 4.0).

The true stress and true strain represent the actual force and deformation experienced by the material, which is crucial for obtaining intrinsic material responses, especially when large geometric changes occur. When an engineering stress–strain curve (i.e., $\sigma_{\text{eng}} - \varepsilon_{\text{eng}}$ curve) or load–elongation curve (i.e., $F - \Delta L$ curve) is obtained from such a tensile test, the resulting relationship typically exhibits non-linear behavior (Fig. 1(b)). This non-linearity can arise from many sources:

**Geometrical non-linearity** arises from changes in a sample's geometry during deformation. In the case of glassy polymers under tensile loading, the cross-sectional area $S$ naturally decreases as the material is stretched. Since true stress is $\sigma = F/S$, a reduction in $S$ leads to an increase in true stress even when $F$ remains constant. In contrast, engineering stress, $\sigma_{\text{eng}} = F/S_0$, does not account for this reduction. As a result, $\sigma_{\text{eng}}$ deviates from the actual stress experienced by the material during deformation.

Furthermore, in experiments where the elongation rate $\dot{L}$ (or engineering strain rate $\dot{\varepsilon}_{\text{eng}} = \dot{L}/L_0$) is held constant, the true strain rate $\dot{\varepsilon} = \dot{L}/L$ decreases as the sample length $L$ increases. This decline in true strain rate can inadvertently affect the material's time-dependent response.

Overall, these geometrical effects introduce non-linearity purely due to changes in the sample's shape during deformation, independent of the material's inherent properties. To minimize such geometrical non-linearities, one may either restrict the analysis to the small-deformation regime, which allows the difference between engineering and true stress–strain to be neglected, or design experiments carefully to capture the true stress–strain relationship.

**Constitutive non-linearity**, in contrast, originates from the intrinsic properties of the glassy polymer and is independent of the sample geometry. The true stress $\sigma$ can exhibit a non-linear relationship with strain (Fig. 1(c)). In a typical true stress–strain curve of a glassy polymer, the material first responds elastically, with stress increasing linearly with strain. As deformation continues, the polymer reaches a yield point, marking the onset of irreversible (plastic) deformation. Beyond this point, the material enters a strain-softening regime, where the stress decreases with increasing strain.[25] This yielding behavior becomes more pronounced when the polymer is aged for a longer period after fabrication,[26] reflecting changes in its microstructure over time. Other non-linear behaviors, such as those associated with strain rate,[27,28] temperature,[29,30] and other thermo-mechanical conditions,[16,31] also play significant roles and will be discussed in the following section. These forms of non-linearity, closely tied to the polymer's molecular architecture, are fundamental to accurate material modeling and characterization.

Additional non-linearities can arise from experimental procedures, particularly during large-deformation or high-strain-rate testing. At high strain rates, rapid deformation may result in adiabatic heating,[32,33] where the heat generated by plastic work is not dissipated efficiently, leading to localized temperature increases. This thermal rise can soften the polymer, introducing deviations from isothermal behavior and contributing to non-linearity. Furthermore, large deformations often lead to strain localization (e.g., necking, shear banding),[34–36] where deformation becomes concentrated in specific regions. This disrupts the uniform strain distribution, making it challenging to control $\dot{\varepsilon}$ by adjusting the overall length change rate $\dot{L}$. These forms of non-linearity are closely linked to material failure mechanisms and are particularly relevant in engineering applications.

In this review, we are only concerned with the intrinsic material response, and thus we do not discuss the effects of geometrical non-linearity, non-uniform deformation, mechanical instability, or failure mechanisms on the mechanical response.

## 3. Behaviors in constant strain rate tests

Constant strain rate (CSR) testing involves deforming a material sample at a precisely controlled, unchanging rate of strain.[37,38] This methodology is paramount in polymer characterization, as it reveals crucial mechanical properties (e.g., elastic modulus, yield stress) and the time-dependent nature of polymers. For accurate characterization, particularly at higher deformation rates or under large deformation, a constant true strain rate is often preferred over an engineering strain rate. Achieving a constant true strain rate typically requires controlling the displacement imposed by the testing machine as an exponential function of time.

CSR tests have been extensively conducted on various amorphous glassy polymers, such as polymethyl methacrylate (PMMA),[39,40] polystyrene (PS),[11,41] polycarbonate (PC),[42,43] epoxy resin,[44,45] and acrylonitrile butadiene styrene (ABS).[46] The tests can also be implemented under diverse deformation modes, including uniaxial tension,[21,47] uniaxial compression,[27,28] shear,[24] and multiaxial loading.[48]

### 3.1. Stress-strain curve

Amorphous glassy polymers exhibit a characteristic non-linear true stress–strain response across a wide range of materials and deformation modes, as illustrated in Fig. 2. The typical features of this response can be broadly divided into several regimes:[49]

(i) In the elastic regime, the true stress $\sigma$ increases linearly with true strain $\varepsilon$ for small strains ($\varepsilon \ll 1$), indicating a reversible deformation. The initial slope of this region defines the elastic modulus.

(ii) As the strain increases, the material enters the anelastic regime, where $\sigma$ begins to deviate from linearity due to time-dependent viscoplasticity. This regime culminates in a local stress maximum, referred to as the (upper) yield stress, occurring at the yield strain, marking the onset of irreversible deformation.

(iii) Following yielding, a strain-softening region is often observed, where the stress decreases with increasing strain.

(iv) The material then transitions into a plastic flow regime, in which the stress plateaus and fluctuates around a nearly constant value, known as the lower yield stress.

(v) At large strains, the material may enter a strain-hardening regime, where the stress begins to rise again with increasing strain.

The area under the stress–strain curve up to the final breaking point corresponds to the material's toughness, a measure of its ability to absorb energy before failure.

The true stress–strain response of a glassy polymer under a given thermal history may not exhibit all the characteristic features shown in Fig. 2. For instance, if the material is rapidly quenched into the glassy state, the post-yield softening may be significantly diminished or absent, leading to a more direct transition from yielding to plastic flow and/or strain hardening.[50]

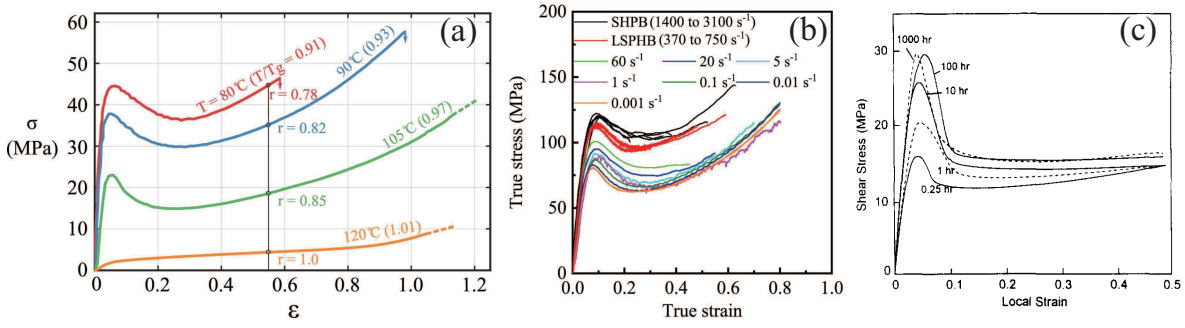



**Fig. 2.** True stress–strain curve in constant strain rate test. (a) Uniaxial tensile behavior of PMMA for a nominal strain rate $\dot{\varepsilon}_{eng} = 5.9 \times 10^{-3}$ s$^{-1}$ at various temperatures (Reproduced from Ref. [23] (CC BY 4.0)), (b) Uniaxial compression behavior of PC at room temperature and different strain rates (Reproduced from Ref. [24] (CC BY 4.0)), (c) Shear behavior of epoxy resin aged at 32.2 °C ($T_g - 10$ °C), sheared at $5 \times 10^{-4}$ s$^{-1}$ for various aging times. (Reproduced from Ref. [24] with permission, Copyright © 1994 Published by Elsevier B.V.)

Subtle differences also arise between different materials and deformation modes. For example, under uniaxial compression, the stress–strain curve generally displays higher yield strength and elastic modulus compared to uniaxial tension.[20,51] Strain hardening is related to molecular weight and chemical crosslinks.[12,52] Lightly crosslinked polymers often do not exhibit significant strain hardening.[53]

### 3.2. Volumetric changes

Amorphous glassy polymers do not remain perfectly volume-conserving during mechanical deformation, as shown in Fig. 3. In uniaxial compression tests, the samples typically undergo volume reduction (densification) in the initial elastic regime. Upon yielding and into the plastic deformation regime, the volume generally remains constant or increases slightly.[54,56,57]

Conversely, in uniaxial tension tests, amorphous glassy polymers typically exhibit a small amount of volume increase (dilatation) in the elastic regime.[31] Some experiments have also observed a volume decrease following the initial dilation, which begins prior to the yield point.[55] Beyond the yield point, significant dilatation may occur, accompanied by the formation of crazing, cavitation, or necking.[58–62]

The volume increase in this regime signifies that the material is becoming discontinuous at a microscopic level due to the creation and nucleation of internal voids. This is different from an "intrinsic" volumetric expansion of the polymer chains themselves, such as thermal expansion, which would imply that the material remains microscopically continuous while uniformly occupying more space.

The microscopic structure of amorphous polymers can be directly probed using advanced techniques such as positron annihilation spectroscopy (PAS).[26,63–65] Ruan *et al.*[66] employed positron annihilation lifetime spectroscopy (PALS) to investigate strain-induced changes in void volume in PC samples subjected to small static tensile deformations (strain $<$ 7%, the yield point of their sample is at about 6% strain). Their results showed that applying strain up to approximately 4% leads to an increase in the average void volume, while the number density of voids remains nearly constant. In the strain range of 4%–7%, no further significant changes in void characteristics were observed. Notably, the total relative increase in void volume with strain was substantially greater than the corresponding increase in bulk volume, as illustrated in Fig. 4. This suggests a non-affine relation between microstructure change and macroscale deformation.

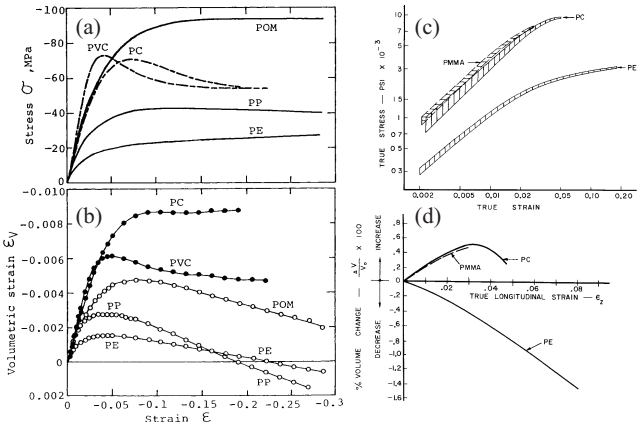



**Fig. 3.** Volume response under constant strain rate loading. (a) and (b) show the stress and volume responses during compression tests, reproduced from Ref. [54] with permission. Copyright © 1988 John Wiley & Sons, Inc. (c) and (d) present the corresponding results for tensile tests before the yielding point, reproduced from Ref. [55] with permission. Copyright © 1972 Society of Plastics Engineers, Inc. Among the materials shown, PVC, PC, and PMMA are amorphous glassy polymers, while POM, PP, and PE are semi-crystalline polymers.

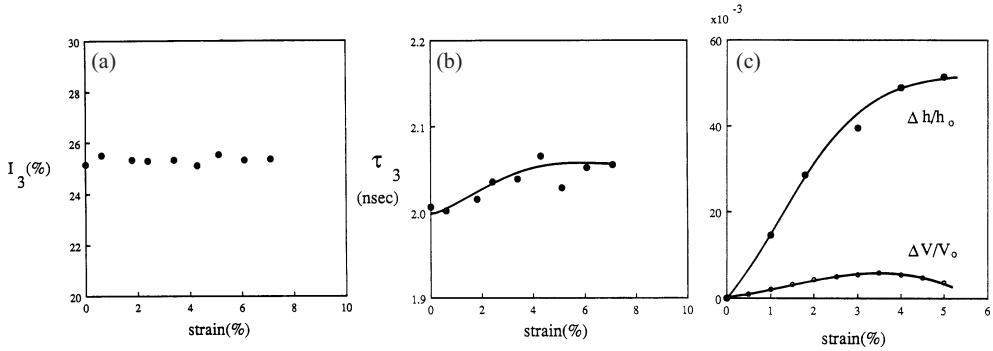



**Fig. 4.** Microscale void volume measured by PALS in a tensile test of PC. (a) o-Ps intensity $I_3$, indicates number density of holes; (b) o-Ps lifetime $\tau_3$, indicates the average hole volume $\langle v_f \rangle$ in the PC sample; (c) the relative change in void volume $h \sim I_3 \langle v_f \rangle$ and macroscopic volume change $V$ from Fig. 3(d). Reprinted with permission from Ref. [66]. Copyright © 1992 American Chemical Society.

Despite these observed densification or dilatation behaviors, the macroscopic true stress–strain curves of amorphous glassy polymers still display a distinct yield point followed by a strain-softening regime. This indicates that the non-linear stress behavior and yielding phenomena are not simply direct consequences of volume change but are instead governed by more complex molecular mechanisms.

### 3.3. Molecular mobility

Molecular mobility refers to the ability of polymer segments to undergo cooperative or localized motions.[67] The molecular mobility can be effectively defined as the inverse of

the segmental relaxation time (relaxation rate). Experiments demonstrate a non-monotonic evolution of molecular mobility parameters during constant strain rate deformation of amorphous glassy polymers.

As the applied strain increases from the initial elastic regime through the yield point and into the stress-softening regime, there is a significant decrease in molecular mobility. Dielectric spectroscopy (DS) experiments can measure the dominant relaxation time ($\tau_\alpha$) and the width of the relaxation time distribution ($w_\tau$). Ciliberto and co-workers[68,69] performed DS measurements in tensile tests on PC, as shown in Fig. 5(a)–5(b). The results showed a reduction in both $\tau_\alpha$ and $w_\tau$. These parameters typically reach a minimum value within the stress-softening regime. This suggests a reduction in the inherent heterogeneity of local environments or relaxation processes that exist in quiescent glasses (known as dynamical heterogeneities), leading to a more uniform response during active plastic flow.

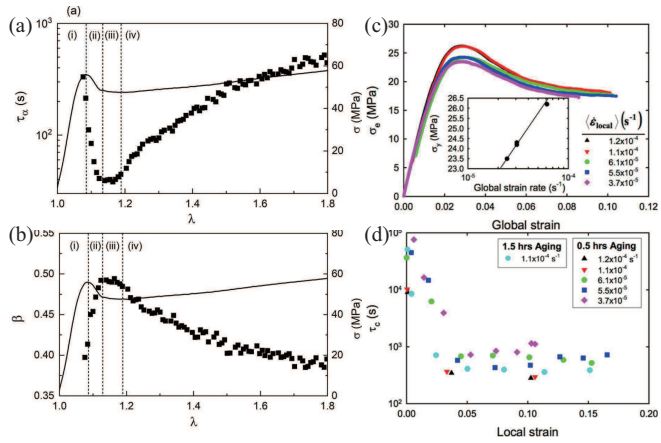



**Fig. 5.** Molecular mobility behavior during a constant strain rate tensile test. (a) and (b) present results from dielectric spectroscopy (DS) measurements conducted during tensile testing of polycarbonate (PC) at an engineering strain rate of $\dot{\lambda} = 2.5 \times 10^{-4}$ s$^{-1}$. In both plots, the solid lines represent the engineering stress (right axis), while the square markers indicate (a) the mean relaxation time $\tau_\alpha$ and (b) the stretching parameter $\beta$ (left axis). A higher value of $\beta$ corresponds to a narrower distribution of relaxation times (i.e., lower $w_\tau$). Reprinted with permission from Ref. [69]. Copyright © 2022 American Chemical Society. (c) and (d) present results obtained using the optical photobleaching method during tensile testing of lightly crosslinked PMMA glasses at 373 K ($T_g - 19$ K), under various engineering strain rates. The corresponding true strain rates in the plastic flow regime are indicated in the legends. (c) Engineering stress–strain curves at different strain rates. The inset shows the dependence of yield stress on the engineering strain rate. (d) Rotational correlation time $\tau_c$ as a function of true strain. Reprinted with permission from Ref. [53]. Copyright © 2014 American Chemical Society.

On the other hand, Ediger and co-workers conducted direct photobleaching measurements in lightly crosslinked PMMA. They also quantified this acceleration (see Figs. 5(c) and 5(d)), showing that the average reorientation time of probe molecules can decrease by as much as two orders of magnitude as the material is brought through yield.[53,70] It also shows that the fastest dynamics are often observed not precisely at the yield peak, but rather within the subsequent stress-softening region.

In the DS experiment of Ciliberto *et al.*, the PC sample exhibits a strain-hardening regime, during which both $\tau_\alpha$ and $w_\tau$ begin to increase again (see Figs. 5(a) and 5(b)). This is a consequence of significant microstructural changes occurring at large strains. As chains become highly stretched and aligned with the deformation direction, their conformational freedom is reduced,[71] leading to increased resistance to further flow and thus longer relaxation times.

By contrast, the lightly crosslinked PMMA exhibits lower toughness relative to PC and does not exhibit strain hardening or the corresponding relaxation time behavior.

The observed non-monotonic evolution of molecular mobility points to a complex interplay of competing mechanisms. The initial acceleration (decrease in $\tau_\alpha$) can be attributed to stress-induced activation of the glassy state, facilitating plastic flow. The subsequent deceleration (increase in $\tau_\alpha$) in the strain-hardening regime suggests the dominance of increasing entropic and enthalpic resistance from highly stretched and oriented polymer chains.

This indicates that the material's properties evolve in a complex manner, reflecting both the immediate response to applied stress and the longer-term structural reorganization.

### 3.4. Toughness and brittleness

Brittleness is the tendency of a glassy polymer to fail through crazing before reaching the yield point. In contrast, ductility describes a polymer's ability to undergo significant plastic deformation and be continuously drawn after yielding without fracturing. The total energy absorbed before fracture, often used as a measure of a material's toughness, can be quantified by the area under the stress–strain curve up to the fracture point.

Wu[72,73] conducted extensive experimental investigations and employed scaling laws to elucidate the intrinsic brittle–ductile behavior of diverse polymers. His analysis demonstrated that the crazing stress ($\sigma_z$) scales with the square root of the entanglement density ($\nu_e$), following the relation $\sigma_z \propto \nu_e^{1/2}$. In contrast, the normalized yield stress ($\{\sigma_y\} = \sigma_y/\delta^2(T - T_g)$) was shown to depend on the intrinsic chain flexibility, being proportional to Flory's characteristic ratio, $\{\sigma_y\} \propto C_\infty$. These chain parameters can be effectively predicted from the molecular architecture of polymers, thereby highlighting the molecular origins of the energy dissipation mechanisms.

Based on the ratio of crazing stress to yield stress ($\sigma_z/\{\sigma_y\}$), polymers can be classified into three categories: *Brittle* polymers tend to fracture mainly by crazing and are inherently brittle. They are characterized by a relatively low entanglement density ($\nu_e <\sim 0.15$ mmol/cm$^3$) and a stiff chain (characteristic ratio $C_\infty >\sim 7.5$). Representative examples include polystyrene (PS) and poly(styrene-acrylonitrile) with acrylonitrile (SAN). *Pseudoductile* polymers are intrinsically

ductile and tend to fracture mainly by yielding. They have a higher entanglement density ($\nu_e >\sim 0.15$ mmol/cm$^3$) and a flexible chain ($C_\infty <\sim 7.5$). The ultimate intrinsic ductility is obtained when $C_\infty \to 2$ for chains with freely rotating joints with tetrahedral skeletal bonds. Examples include polycarbonate (PC) and poly(ethylene terephthalate) (PET). *Intermediate* polymers exhibit a transitional behavior, having comparable crazing and yield stresses. This occurs when the entanglement density is approximately 0.15 mmol/cm$^3$ and the characteristic ratio is around 7.5. Typical examples include poly(methyl methacrylate) (PMMA) and poly(vinyl chloride) (PVC).

Table 1 summarizes the ductile–brittle behavior of several typical polymers.

**Table 1.** Brittle-ductile behavior of typical polymers. Reprinted with permission from Ref. [72]. Copyright © 1992 Society of Chemical Industry.

| Polymer | $\nu_e$ (mmol/cm$^3$) | $C_\infty$ | Type of polymer | Mechanism in neat polymer |
|---|---|---|---|---|
| PS | 0.06 | 10.8 | Brittle | Craze |
| SAN30 | 0.10 | 9.3 | | |
| PMMA | 0.13 | 8.2 | Intermediate | |
| PVC | 0.25 | 7.6 | | |
| N66 | 0.54 | 6.1 | Pseudoductile | |
| PET | 0.82 | 4.2 | | |
| PC | 0.67 | 2.4 | | Yield |
| Ultimate ductility | - | 2.0 | | |

Over the past three decades, the classical scaling framework has been substantially extended through controlled experiments, molecular simulations, and micromechanical modeling. Molecular dynamics (MD) simulations by Hoy *et al.*[74] revealed that the traditional assumption of inherent brittleness in semi-flexible polymer glasses (SPG) is incomplete; the contribution of stretched Kuhn segments to stress transmission was previously underestimated, leading to the observation of unexpected ductility in these systems. Zhao *et al.*[71] further established, via large-scale MD simulations, that fracture behavior is strongly correlated with molecular conformations. Specifically, the narrowing of conformational distributions prior to crack propagation reflects reduced configurational freedom and precedes failure. Suo *et al.*[75–77] demonstrated that polymer networks with entanglement densities far exceeding their crosslink densities exhibit significantly enhanced toughness, as load transfer occurs predominantly through entanglements that distribute mechanical energy across many chains and over large volumes before any bond rupture.

In parallel, Chen *et al.*[78] showed that introducing dynamic covalent and hydrogen-bonding interactions enables energy dissipation via reversible bond exchange, a finding consistent with the results of Meng *et al.*[79,80] and Zheng *et al.*,[8] who reported similar toughening mechanisms in dynamically cross-linked polymer networks.

## 4. Influence of experimental conditions

### 4.1. Strain rate and temperature

Amorphous glassy polymers exhibit a pronounced sensitivity to both strain rate and temperature. The pre-yield behavior of amorphous glassy polymers is typically characterized by their initial elastic modulus (stiffness). As temperature increases, particularly approaching the glass transition temperature ($T_g$), the elastic modulus decreases significantly, marking a transition from a stiff, glassy state to a compliant, rubbery regime.[40,81–83] For example, the elastic modulus of PMMA decreased by 73.9% within the studied range of 20 °C to 80 °C.[84]

The yield stress of amorphous glassy polymers generally increases with increasing strain rate and decreases with increasing temperature.[30,40,85–92] For instance, the yield stress of PMMA has been experimentally observed to decrease by approximately 67.7% as the temperature rises from room temperature to 80 °C.[84] On the other hand, yield stress increases with strain rate, typically following a nearly linear relationship with the logarithm of strain rate over several orders of magnitude.[93] However, the strain-rate sensitivity of yield stress varies significantly among different amorphous polymers. For example, PLA exhibits a much higher rate sensitivity (approximately ±14 MPa per decade at 37 °C) compared to PC or poly(ether ether ketone) (PEEK), which display a lower sensitivity of about 3–4 MPa per decade.[94]

Over broader ranges of strain rate and temperature, deviations from the simple log-linear behavior may occur, often marked by an inflection point in the yield stress response, as illustrated in Fig. 6. Such changes in slope have been correlated with dynamic mechanical thermal analysis (DMTA) results and are associated with the onset of multiple molecular relaxation processes (often referred to as $\alpha$ and $\beta$ relaxations) in polymeric glasses.[95]

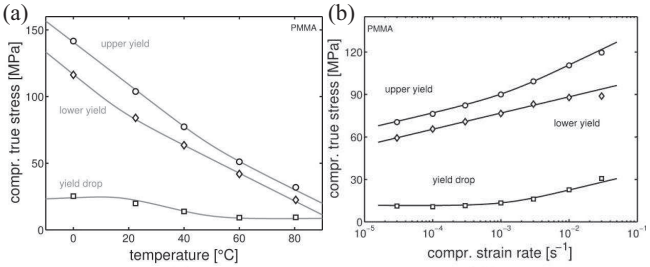



**Fig. 6.** Temperature and strain rate dependence of yield behavior in compressive constant strain rate tests of PMMA. (a) Yield stress (i.e., upper yield stress), flow stress (i.e., lower yield stress), and yield drop as functions of temperature at a true strain rate of $10^{-3}$ s$^{-1}$. (b) Corresponding dependence of these quantities on true strain rate at a fixed temperature of 22 °C. Reprinted with permission from Ref. [95]. Copyright © 2011 Wiley Periodicals, Inc.

The post-yield behavior of amorphous polymers, which includes strain softening, plastic flow, and strain hardening, is also sensitive to both strain rate and temperature. The stress required to sustain plastic flow (lower yield stress) exhibits

a similar qualitative dependence on strain rate and temperature as the upper yield stress, although the respective inflection points may differ.[95] Consequently, when the rate-induced increase in upper yield stress exceeds that of the flow stress, the extent of post-yield strain softening tends to increase with strain rate. Conversely, if the lower yield stress merely translates along the strain-rate axis, the magnitude of the yield drop during the strain-softening regime remains effectively independent of strain rate.

The time-dependent mechanical response of amorphous glassy polymers exhibits a strong empirical equivalence between increasing strain rate and decreasing temperature. This relationship reflects the underlying viscoelastic nature of polymers. The time-temperature superposition principle (TTSP)[96,97] postulates that the effects of observation time (equivalent to the inverse of strain rate in CSR tests) and temperature on viscoelastic properties can be superimposed through horizontal shifting of data along the logarithmic time or frequency axis. By conducting experiments at different temperatures and applying appropriate shift factors, a single, smooth master curve can be constructed. This master curve captures the mechanical response over a wide range of effective timescales, allowing low strain rate data at elevated temperatures to be used to predict high-rate behavior at lower temperatures.[85]

For instance, dielectric spectroscopy studies on PC[68] show that the relaxation spectrum of a deformed polymer at room temperature can be shifted to match the spectrum of the undeformed polymer measured at an effective temperature $T_a$ slightly below the glass transition temperature $T_g$. At this temperature, the dominant segmental relaxation time $\tau_\alpha(T_a)$ of quiescent PC is observed to scale inversely with the applied strain rate $\dot{\gamma}$, i.e., $\tau_\alpha(T_a) \sim 1/\dot{\gamma}$. This result reinforces the TTSP framework and demonstrates how temperature and strain rate act as equivalent variables in dictating polymer relaxation dynamics and mechanical response.

### 4.2. Pressure

The mechanical properties of glassy polymers are sensitive to hydrostatic pressure (abbreviated as pressure).[18,98] The pressure is obtained from the decomposition of the stress tensor. In analyzing pressure effects, the stress is typically expressed in tensor form to account for forces acting in all directions, and pressure is defined as the isotropic stress. The stress tensor can be decomposed into two components, $\boldsymbol{\sigma} = \boldsymbol{\sigma}^{\mathrm{vol}} + \boldsymbol{\sigma}^{\mathrm{dev}}$, where $\boldsymbol{\sigma}^{\mathrm{vol}} = \frac{1}{3}\,\mathrm{tr}(\boldsymbol{\sigma})\,\boldsymbol{I}$ denotes the isotropic (or volumetric) part of the stress, and $\boldsymbol{\sigma}^{\mathrm{dev}} = \boldsymbol{\sigma} - \boldsymbol{\sigma}^{\mathrm{vol}}$ represents the deviatoric (trace-free) part. The term "(hydrostatic) pressure" refers to the magnitude of the isotropic stress, given by $p = -\frac{1}{3}\,\mathrm{tr}(\boldsymbol{\sigma})$, where the negative sign reflects the convention that hydrostatic pressure acts inward on an object. The term "octahedral stress" refers to the magnitude of shear stress, given by $\tau^{\mathrm{oct}} = \left(\boldsymbol{\sigma}^{\mathrm{dev}} : \boldsymbol{\sigma}^{\mathrm{dev}}\right)^{1/2}$.

The elastic stiffness of amorphous glassy polymers increases under hydrostatic compression. Experimental studies show that applying confining pressure raises the instantaneous moduli. For example, static compression tests on an epoxy resin demonstrated that its compressive Young's modulus increased significantly with applied pressure.[44] As shown in Fig. 7, the compressive modulus increased by 20–40% as pressure was raised to a few hundred MPa. Similarly, measurements on PC, PMMA, and amorphous PET also indicate that their tensile moduli increase with pressure.[99,100]

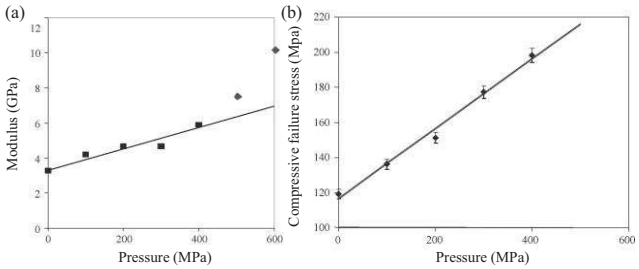



**Fig. 7.** Pressure dependence of epoxy resin on its (a) elastic modulus and (b) yield stress. Reprinted with permission from Ref. [44]. Copyright © 2004 Elsevier Ltd.

The yield criterion defines the limit of elastic behavior in a material (i.e., the transition from purely elastic deformation to plastic deformation) under any combination of stresses. In glassy polymers, the yield stress depends strongly on hydrostatic pressure.[42,46,101,102] This differs from the standard von Mises or Tresca models, which assume no hydrostatic pressure dependence.

Quasi-static experiments report that yield strength (in both tension and compression) tends to increase approximately linearly with confining pressure. For example, tests on PMMA show that its tensile yield stress increases as pressure is applied.[39,89,103] Likewise, epoxy under compression exhibits higher peak stress under pressure[44] (Fig. 7(b)).

Notably, compressive and tensile yields shift in opposite directions under pressure: positive (compressive) hydrostatic stress increases the yield stress, while negative (tensile) hydrostatic stress decreases it. PVC demonstrates a clear distinction between its tensile and compressive yield strengths due to this pressure dependence.[20] The ratios of compressive to tensile yield strength for various polymeric materials typically range between 1 and 1.4.

The pressure-dependent yield behavior can be accurately described by pressure-modified von Mises or Tresca criteria,[104,105] where the equivalent shear stress at yield, $\tau_y^{\mathrm{oct}}$, scales linearly with isotropic stress

$$\tau_y^{\mathrm{oct}} = \tau_0 + \mu p.$$

Here, $\mu$ is a material constant determined experimentally, and $\tau_0$ is the shear yield stress at zero hydrostatic pressure.

Complementing these findings, researchers have successfully mapped the yield behavior of glassy polymers using the Drucker–Prager criterion.[106]

### 4.3. Thermal history

The mechanical behavior of amorphous glassy polymers is influenced not only by the instantaneous conditions but also by their prior thermal and mechanical histories. Quenching involves rapidly cooling the polymer from above its glass transition temperature ($T_g$) to a temperature well below $T_g$. Annealing refers to holding a polymer isothermally for an extended period to allow structural relaxation. When a glassy polymer is annealed below its glass transition temperature ($T_g$), it spontaneously undergoes a time-dependent evolution toward equilibrium, a process known as physical aging. During aging, the polymer gradually densifies as excess free volume and enthalpy are reduced, leading to increased stiffness and yield stress but decreased ductility and segmental mobility. Rejuvenation denotes the process of reversing or eliminating the effects of aging or annealing by introducing excess free volume and disorder into the glassy structure.

The thermal history applied to a polymer can significantly modify the overall shape of its stress–strain curve. Freshly quenched glassy polymers show lower yield stress and a less pronounced yielding peak. Long-term aging below the glass transition temperature ($T_g$) stiffens glassy polymers and increases their yield stress,[107,108] as shown in Fig. 8. For example, in polylactic acid (PLA) aged at room temperature, the yield stress was observed to increase and reach a plateau after approximately 1000 hours.[109] Nanzai *et al.*[110,111] investigated the evolution of the elastic modulus and yield stress with aging time in a series of aged PMMA specimens. They reported that both the elastic modulus and yield stress increased with aging time. Moreover, the slope of the elastic modulus versus log(aging time) for specimens aged under strain was much steeper than that for quiescently aged specimens.[112]

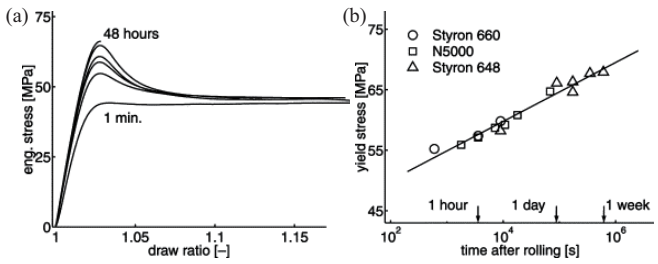



**Fig. 8.** Effect of aging time on the tensile stress–strain behavior of polystyrene (PS) under a constant engineering strain rate of $10^{-3}$ $s^{-1}$ at room temperature. (a) Engineering stress–strain curves for different aging times. (b) Yield stress as a function of aging time. Reprinted with permission from Ref. [50]. Copyright © 2002 Elsevier Science Ltd.

In contrast, at large strains, the effects of thermal history and physical aging are effectively "erased".[113] For both PMMA and PC, the stress–strain curves in the plastic flow and strain-hardening regimes converge to a single curve, regardless of aging time.[24,26] This phenomenon is referred to as deformation-induced rejuvenation.[114]

The thermal history significantly influences the structural relaxation behavior of glassy polymers. When a polymer is rapidly cooled from above its glass transition temperature ($T_g$) to below $T_g$, its molecular chains become kinetically trapped in a non-equilibrium, disordered configuration containing a certain amount of free space (i.e., free volume).[31,63]

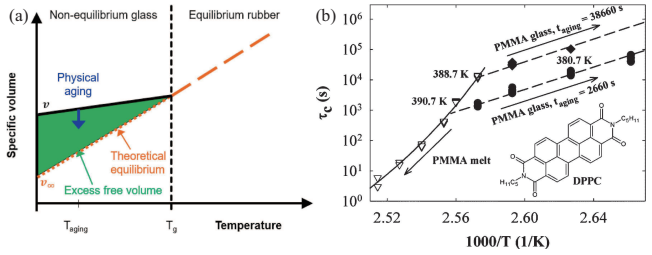



**Fig. 9.** Effect of aging time on the microstructure of glassy polymers. (a) Schematic representation of the volume–temperature behavior of a glassy polymer. Reprinted with permission from Ref. [115]. Copyright © 2020 Elsevier Ltd. (b) Temperature dependence of relaxation time for lightly cross-linked PMMA. Reprinted with permission from Ref. [114]. Copyright © 2010 American Chemical Society.

As illustrated in Fig. 9(a), upon quenching from a temperature above $T_g$ to below it, the specific volume of the polymer follows the path indicated by the orange dashed and solid blue lines. The orange dotted line below $T_g$ represents an extrapolation of the equilibrium rubbery-state specific volume and corresponds to the hypothetical equilibrium specific volume in the glassy state. However, due to the extremely low molecular mobility of polymers below $T_g$, this equilibrium state is not readily attained.

The difference between the actual and equilibrium specific volumes is the free volume, shown as the green-shaded area. During physical aging, the polymer chains gradually rearrange and become more efficiently packed, resulting in a reduction in free volume.[115–118] This densification manifests as a gradual shrinkage of the material. The dark blue arrow in Fig. 9(a) indicates the direction of physical aging, representing the slow progression of specific volume toward thermodynamic equilibrium.

The reduction in free volume directly impedes the segmental mobility of polymer chains, leading to an increase in the characteristic relaxation times.[114] This inverse relationship between free volume and relaxation dynamics is evidenced by comparing the relaxation time behavior in Fig. 9(b) and the volume behavior shown in Fig. 9(a). As the temperature decreases from above $T_g$, the specific volume declines while the relaxation time increases, with both exhibiting a notable transition near the glass transition temperature.

Moreover, in Fig. 9(b), the relaxation time of PMMA after an aging period of 38660 s is approximately an order of magnitude longer than that of a sample aged for only 2660 s.

This increase in relaxation time corresponds to the gradual densification observed in Fig. 9(a), where the more extensively aged sample exhibits a lower specific volume due to continued physical aging.

## 5. Perspectives

Amorphous glassy polymers exhibit rich and complex non-linear mechanical behavior under CSR testing, reflecting the interplay between their molecular structure, thermodynamic state, and external loading conditions. This review has summarized key experimental findings related to stress–strain responses, volume evolution, molecular mobility, toughness and brittleness, and examined how these features are influenced by factors such as strain rate, temperature, hydrostatic pressure, and thermal history. By focusing exclusively on CSR testing, we have highlighted the characteristic deformation mechanisms unique to amorphous glassy polymers and the critical role of testing conditions in shaping their mechanical response.

The mechanical response of amorphous glassy polymers is distinct from other materials.

Semi-crystalline glassy polymers exhibit more complex constant strain rate behavior, primarily due to the orientation and deformation of anisotropic crystalline domains. These differences are particularly evident in the associated volume changes, as illustrated in Fig. 3.

In contrast, rubbers display a much larger range of recoverable deformation, characterized by the coupled contributions of entropy-driven hyperelasticity and viscoelasticity.[119,120] Unlike glassy polymers, the elastic modulus of rubbers increases with temperature, reflecting the entropic nature of their deformation.[121,122]

Metals differ further in that their load–elongation curves often exhibit two distinct stress peaks,[25] with the first associated with the burst of plastic deformation induced by dislocation mechanisms and mechanical twinning, and the second with cross-sectional area reduction from necking.

To elucidate these unique behaviors, various microscopic mechanisms have been proposed. Temperature effects are commonly described by the Arrhenius relation ($\tau \sim \exp(E_a/(RT))$), which introduces activation energy into the understanding of molecular mobility,[38] and by the Williams–Landel–Ferry (WLF) equation, which captures the time–temperature superposition arising from cooperative chain motions.[96] To address the influence of stress, the Eyring model[123] attributes molecular activation to stress-induced modifications of energy barriers, while the Argon model[124] emphasizes the enhanced motion and rearrangement of chain kinks. Molecular mobility in glassy polymers also exhibits memory effects during annealing and physical aging, which are often represented through internal variables that accumulate thermodynamic history.[125]

Based on these insights, multiscale rheological models have been developed. At the segmental level, the Chen–Schweizer model[126,127] introduced the above mechanisms into a Langevin equation framework to describe the evolution of segmental relaxation and reproduce characteristic stress–strain behavior. At the macroscopic level, continuum constitutive models incorporating molecular mobility have led to various large-deformation viscoelastic theories.[128–137] Combined with variational and finite element methods,[138] these models enable quantitative predictions of stress and deformation in complex geometries, providing reliable tools for engineering applications.

However, capturing all these behaviors across different regimes often requires distinct assumptions. Current interpretations rely on empirical or semi-empirical models involving numerous fitting parameters. There is still a lack of a unified theoretical framework that cohesively describes the full spectrum of non-linear responses while maintaining consistency across temperature, strain rate, and pressure dependencies.

Such efforts will be crucial for enabling predictive modeling and rational microstructural design strategies to enhance strength, toughness, and damage tolerance. For instance, incorporating dynamic noncovalent interactions[78] can introduce stress-activated softening and energy dissipation through reversible bond breakage and reformation. Tailoring network architecture and chain topology[139] may also promote synergistic deformation mechanisms while delaying catastrophic failure. Ample opportunities exist for investigation and innovation.

## Acknowledgements

This work was supported in part by the National Natural Science Foundation of China (Grant Nos. 22473005, 21961142020, and 21822302), the Fundamental Research Funds for the Central Universities (Grant No. YWF-22-K-101), and the Guangdong Provincial Key Laboratory of Special Engineering Plastics (Enterprise) (Grant No. 2023B1212070027). The authors also acknowledge the support of the High-Performance Computing Center of Beihang University.

## References

[1] Roy A, Venna S R, Rogers G, Tang L, Fitzgibbons T C, Liu J, McCurry H, Vickery D J, Flick D and Fish B 2021 *Proc. Natl. Acad. Sci. USA* **118** e2022194118

[2] Ghosal K and Freeman B D 1994 *Polym. Adv. Technol.* **5** 673

[3] Xin X, Lin C, Wang X, Liu F, Dong L, Liu L, Liu Y and Leng J 2025 *Mater. Futures* **4** 012402

[4] Luo L, Zhang F, Wang L, Liu Y and Leng J 2024 *Adv. Funct. Mater.* **34** 2312036

[5] Zhang J, Xu Y, An S, Sun Y, Li X and Li Y 2020 *Chin. Phys. B* **29** 076202
[6] Lendlein A and Kelch S 2002 *Angew. Chem.-Int. Edit.* **41** 2034
[7] Wang M, Xiao X, Siddika S, Shamsi M, Frey E, Qian W, Bai W, O'Connor B T and Dickey M D 2024 *Nature* **631** 313
[8] Zhang X N, Wang Y J, Sun S, Hou L, Wu P, Wu Z L and Zheng Q 2018 *Macromolecules* **51** 8136
[9] Pan J, Zhang W, Zhu J, Tan J, Huang Y, Mo K, Tong Y, Xie Z, Ke Y, Zheng H, Ouyang H, Shi X and Gao L 2023 *Adv. Mater.* **35** 2207750
[10] Wang Y, Hou Y, Vyas C, Huang B and Bartolo P 2025 *Mater. Futures* **4** 025401
[11] Liu J, Lin P, Li X and Wang S Q 2015 *Polymer* **81** 129
[12] Wendlandt M, Tervoort T A and Suter U W 2005 *Polymer* **46** 11786
[13] Mohammadi M, Fazli H, karevan M and Davoodi J 2017 *Eur. Polym. J.* **91** 121
[14] Palczynski K, Wilke A, Paeschke M and Dzubiella J 2017 *Phys. Rev. Mater.* **1** 043804
[15] Cangialosi D 2024 *J. Polym. Sci.* **62** 1952
[16] Song H, Medvedev G A, Caruthers J M, Young Jo J and Kim J 2023 *Polymer* **268** 125707
[17] Gibhardt D, Krauklis A E, Doblies A, Gagani A, Sabalina A, Starkova O and Fiedler B 2023 *Polym. Test* **118** 107901
[18] Hoppel C P R, Bogetti T A and Gillespie J W 1995 *J. Thermoplast. Compos. Mater.* **8** 375
[19] Sudharshan Phani P, Hackett B, Walker C, Oliver W and Pharr G 2023 *Curr. Opin. Solid State Mat. Sci.* **27** 101054
[20] Siviour C R and Jordan J L 2016 *J. Dyn. Behav. Mater.* **2** 15
[21] Van Loock F and Fleck N A 2018 *Polymer* **148** 259
[22] Brinson H F and Brinson L C 2015 *Stress and Strain Analysis and Measurement* (Boston: Springer US) pp. 15–55
[23] Song P, Trivedi A R and Siviour C R 2023 *Polym. Test* **121** 107986
[24] Aboulfaraj M, G'sell C, Mangelinck D and McKenna G 1994 *J. Non-Cryst. Solids* **172-174** 615–621
[25] Brown N and Ward I M 1968 *J. Polym. Sci. Pt. A-2 Polym. Phys.* **6** 607
[26] Hasan O, Boyce M, Li X and Berko S 1993 *J. Polym. Sci. Pt. B-Polym. Phys.* **31** 185
[27] Dar U A, Zhang W, Xu Y and Wang J 2014 *J. Polym. Res.* **21** 519
[28] Liu F, Wang J, Long S, Zhang H and Yao X 2022 *Mech. Mater.* **167** 104246
[29] Arruda E M, Boyce M C and Jayachandran R 1995 *Mech. Mater.* **19** 193
[30] Richeton J, Ahzi S, Vecchio K S, Jiang F C and Adharapurapu R R 2006 *Int. J. Solids Struct.* **43** 2318
[31] Brady T E and Yeh G S Y 1971 *J. Appl. Phys.* **42** 4622
[32] Rittel D 1999 *Mech. Mater.* **31** 131
[33] Ward I and Sweeney J 2012 *Yielding and Instability in Polymers* (John Wiley & Sons, Ltd) Chap. 12, pp. 319–378
[34] van Melick H, Govaert L and Meijer H 2003 *Polymer* **44** 3579
[35] Cheng S and Wang S Q 2013 *Phys. Rev. Lett.* **110** 065506
[36] Zhang R, Bai P, Lei D and Xiao R 2018 *Int. J. Solids Struct.* **146** 203
[37] Bowden P B 1973 *The Yield Behaviour of Glassy Polymers* (Dordrecht: Springer Netherlands) pp 279–339
[38] Caruthers J M and Medvedev G A 2016 *Polymer Glasses* (CRC Press) pp 123–194
[39] Zhang L, Townsend D, Petrinic N and Pellegrino A 2021 *Int. J. Impact Eng.* **158** 104026
[40] Cheng W M, Miller G A, Manson J A, Hertzberg R W and Sperling L H 1990 *J. Mater. Sci.* **25** 1917
[41] Bukowski C, Zhang T, Riggleman R A and Crosby A J 2021 *Sci. Adv.* **7** eabg9763
[42] Wohlford A, Walter T, Casem D, Moy P and Kidane A 2019 *Dynamic Behavior of Materials, Volume 1* ed Kimberley J, Lamberson L E and Mates S (Cham: Springer International Publishing) pp. 259–262
[43] Dreistadt C, Bonnet A S, Chevrier P and Lipinski P 2009 *Mater. Des.* **30** 3126
[44] Hine P, Duckett R, Kaddour A, Hinton M and Wells G 2005 *Composites Part A: Applied Science and Manufacturing* **36** 279
[45] Gu J, Bai Y, Zhao Z and Zhang C 2024 *Polymer* **295** 126744
[46] Verbeeten W M H, Sánchez-Soto M and Maspoch M L 2022 *J. Appl. Polym. Sci.* **139** 52295
[47] Fu S, Wang Y and Wang Y 2009 *Polym. Test* **28** 724
[48] Kim J W, Medvedev G A and Caruthers J M 2013 *Polymer* **54** 2821
[49] Hoy R S 2011 *J. Polym. Sci. Pt. B-Polym. Phys.* **49** 979
[50] van Melick H, Govaert L, Raas B, Nauta W and Meijer H 2003 *Polymer* **44** 1171
[51] Boyce M C and Arruda E M 1990 *Polym. Eng. Sci.* **30** 1288
[52] Govaert L E and Tervoort T A 2004 *J. Polym. Sci. Pt. B-Polym. Phys.* **42** 2041
[53] Bending B, Christison K, Ricci J and Ediger M D 2014 *Macromolecules* **47** 800
[54] Kitagawa M and Yoneyama T 1988 *J. Polym. Sci. Part C: Polymer Letters* **26** 207
[55] Powers J M and Caddell R M 1972 *Polym. Eng. Sci.* **12** 432
[56] Pampillo C A and Davis L A 1971 *J. Appl. Phys.* **42** 4674
[57] Whitney W and Andrews R D 1967 *J. Polym. Sci. Part C: Polymer Symposia* **16** 2981
[58] Cross A, Haward R and Mills N 1979 *Polymer* **20** 288
[59] Rottler J and Robbins M O 2003 *Phys. Rev. E* **68** 011801
[60] Volynskii A L, Yarysheva A Y, Rukhlya E G, Efimov A V, Yarysheva L M and Bakeev N F 2013 *Russ. Chem. Rev.* **82** 988
[61] Shabahang S, Tao G, Kaufman J J, Qiao Y, Wei L, Bouchenot T, Gordon A P, Fink Y, Bai Y, Hoy R S, *et al.* 2016 *Nature* **534** 529
[62] Andersen M, Hopperstad O S and Clausen A H 2019 *Strain* **55** e12314
[63] Hutchinson J M 1995 *Prog. Polym. Sci.* **20** 703
[64] Hagiwara K, Ougizawa T, Inoue T, Hirata K and Kobayashi Y 2000 *Radiat. Phys. Chem.* **58** 525
[65] Guo H, Luo M, Dong Y, Yang E, Huang D, Ye B, Zhang H, Li L and Cui K 2025 *Macromolecules* **58** 4645
[66] Ruan M Y, Moaddel H, Jamieson A M, Simha R and McGervey J D 1992 *Macromolecules* **25** 2407
[67] Padhye N 2021 *Physics of Deformation in Polymer Glasses and Deformation-Induced Molecular Mobility* (Cham: Springer International Publishing) pp. 35–57
[68] Pérez-Aparicio R, Cottinet D, Crauste-Thibierge C, Vanel L, Sotta P, Delannoy J Y, Long D R and Ciliberto S 2016 *Macromolecules* **49** 3889
[69] Hem J, Crauste-Thibierge C, Merlette T C, Clément F, Long D R and Ciliberto S 2022 *Macromolecules* **55** 9168
[70] Lee H N, Paeng K, Swallen S F and Ediger M D 2009 *Science* **323** 231
[71] Zhao W, Jain Y, Müller-Plathe F, Steinmann P and Pfaller S 2024 *J. Mech. Phys. Solids* **193** 105884
[72] Wu S 1992 *Polym. Int.* **29** 229
[73] Wu S 1990 *Polym. Eng. Sci.* **30** 753
[74] Dietz J D, Nan K and Hoy R S 2022 *Phys. Rev. Lett.* **129** 127801
[75] Kim J, Zhang G, Shi M and Suo Z 2021 *Science* **374** 212
[76] Nian G, Kim J, Bao X and Suo Z 2022 *Adv. Mater.* **34** 2206577
[77] Steck J, Ahn C H and Suo Z 2025 *Ann. Rev. Mater. Res.* **55** 333
[78] Yang H, Wu S and Chen Q 2025 *Polym. Sci. Technol.* **1** 261
[79] Meng F, Saed M O and Terentjev E M 2022 *Nat. Commun.* **13** 5753
[80] Zhao J and Meng F 2023 *Phys. Rev. Lett.* **131** 068101
[81] Wu Y, Peng L, Cui Y and Fan S 2023 *J. Mater. Civ. Eng.* **35** 04023377
[82] Agrawal S, Patidar D, Dixit M, Sharma K and Saxena N S 2010 *AIP Conf. Proc.* **1249** 79
[83] Lei K F, Li W J and Yam Y 2005 *Microsyst. Technol.* **11** 353
[84] Abdel-Wahab A A, Ataya S and Silberschmidt V V 2017 *Polym. Test* **58** 86
[85] Kendall M J and Siviour C R 2014 *Phil. Trans. R. Soc. A.* **372** 20130202
[86] Jordan J L, Spowart J E, Kendall M J, Woodworth B and Siviour C R 2014 *Phil. Trans. R. Soc. A.* **372** 20130215
[87] Moy P, Gunnarsson C A, Weerasooriya T and Chen W 2011 *Dynamic Behavior of Materials, Volume 1* ed Proulx T (New York, NY: Springer New York) pp. 125–133
[88] Li Z and Lambros J 2001 *Int. J. Solids Struct.* **38** 3549
[89] Duckett R, Rabinowitz S and Ward I 1970 *J. Mater. Sci.* **5** 909
[90] Bauwens-Crowet C, Bauwens J C and Homès G 1969 *J. Polym. Sci. Pt. A-2 Polym. Phys.* **7** 735
[91] Roetling J 1965 *Polymer* **6** 311
[92] Hu W, Guo H, Chen Y, Xie R, Jing H and He P 2016 *Eur. Polym. J.* **85** 313
[93] Jordan J L, Siviour C R and Woodworth B 2012 *AIP Conf. Proc.* **1426** 191
[94] Engels T A, Söntjens S H, Smit T H and Govaert L E 2010 *J. Mater. Sci.: Mater. Med.* **21** 89
[95] van Breemen L C A, Engels T A P, Klompen E T J, Senden D J A and Govaert L E 2012 *J. Polym. Sci. Pt. B-Polym. Phys.* **50** 1757

[96] Rubinstein M and Colby R H 2003 *Polymer Physics* (Oxford University Press)
[97] Osswald T A 2017 *Understanding Polymer Processing (Second Edition)* ed. Osswald T A (Hanser) pp. 29–59 Second Edition
[98] Pae K D and Bhateja S K 1975 *J. Macromol. Sci. Pt. C* **13** 1
[99] Christiansen A W, Baer E and Radcliffe S V 1971 *Philos. Mag.* **24** 451
[100] Ainbinder S B, Laka M G and Maiors I Y 1965 *Mech. Compos. Mater.* **1** 50
[101] Radcliffe S V 1973 *Effects of Hydrostatic Pressure on the Deformation and Fracture of Polymers* (Boston, MA: Springer US) pp. 191–209
[102] Matsushige K, Radcliffe S V and Baer E 1975 *J. Mater. Sci.* **10** 833
[103] Rittel D and Brill A 2008 *J. Mech. Phys. Solids* **56** 1401
[104] Quinson R, Perez J, Rink M and Pavan A 1997 *J. Mater. Sci.* **32** 1371
[105] Caddell R, Raghava R and Atkins A 1974 *Mater. Sci. Eng.* **13** 113
[106] Seltzer R, Cisilino A P, Frontini P M and Mai Y W 2011 *Int. J. Mech. Sci.* **53** 471
[107] Meijer H E and Govaert L E 2005 *Prog. Polym. Sci.* **30** 915
[108] Rottler J and Robbins M O 2005 *Phys. Rev. Lett.* **95** 225504
[109] Gamez-Perez J, Velazquez-Infante J C, Franco-Urquiza E, Pages P, Carrasco F, Santana O O and Maspoch M L 2011 *Express Polym. Lett.*
[110] Nanzai Y, Miwa A and Cui S Z 2000 *Polym. J.* **32** 51
[111] Gui S Z and Nanzai Y 2001 *Polym. J.* **33** 444
[112] Razavi M, Xing E and Ediger M D 2022 *Macromolecules* **55** 10043
[113] McKenna G B 2003 *J. Phys.-Condes. Matter* **15** S737
[114] Lee H N and Ediger M D 2010 *Macromolecules* **43** 5863
[115] Merrick M M, Sujanani R and Freeman B D 2020 *Polymer* **211** 123176
[116] Huang Y, Wang X and Paul D 2006 *J. Membr. Sci.* **277** 219
[117] Hill A J and Tant M R 1999 *The Structure and Properties of Glassy Polymers* (American Chemical Society) chap 1, pp. 1–20
[118] Kovacs A J 1964 Transition vitreuse dans les polymères amorphes. etude phénoménologique *Fortschritte Der Hochpolymeren-Forschung* (Berlin, Heidelberg: Springer Berlin Heidelberg) pp. 394–507
[119] Treloar L G 1975 *The Physics of Rubber Elasticity* (OUP Oxford)
[120] Shim V, Yang L, Lim C and Law P 2004 *J. Appl. Polym. Sci.* **92** 523
[121] Anthony R L, Caston R H and Guth E 1942 *J. Phys. Chem.* **46** 826
[122] Cam J B L 2010 *Rubber Chem. Technol.* **83** 247
[123] Eyring H 1936 *J. Chem. Phys.* **4** 283
[124] Argon A S 1973 *Philos. Mag.* **28** 839
[125] Medvedev G A, Xing E, Ediger M D and Caruthers J M 2022 *Macromolecules* **55** 6351
[126] Chen K, Saltzman E J and Schweizer K S 2010 *Annu. Rev. Condens. Matter Phys.* **1** 277
[127] Chen K and Schweizer K S 2011 *Macromolecules* **44** 3988
[128] Haward R N, Thackray G and Sugden T M 1968 *Proc. R. Soc. London Ser. A-Math. Phys. Eng. Sci.* **302** 453
[129] Boyce M C, Parks D M and Argon A S 1988 *Mech. Mater.* **7** 15
[130] Wu P and van der Giessen E 1995 *Int. J. Plast.* **11** 211
[131] Buckley C and Jones D 1995 *Polymer* **36** 3301
[132] Govaert L E, Timmermans P H M and Brekelmans W A M 1999 *J. Eng. Mater. Technol.-Trans. ASME* **122** 177
[133] Richeton J, Ahzi S, Vecchio K, Jiang F and Makradi A 2007 *Int. J. Solids Struct.* **44** 7938
[134] Anand L, Ames N M, Srivastava V and Chester S A 2009 *Int. J. Plast.* **25** 1474
[135] Fielding S M, Larson R G and Cates M E 2012 *Phys. Rev. Lett.* **108** 048301
[136] Lan T, Jiang Y and Wu P 2022 *Polymer* **240** 124524
[137] Xiao R, Tian C, Xu Y and Steinmann P 2022 *Int. J. Plast.* **156** 103361
[138] Farias J M C, Stainier L and Fancello E A 2020 *Continuum Mech. Thermodyn.* **32** 1037
[139] Masubuchi Y, Doi Y, Ishida T, Sakumichi N, Sakai T, Mayumi K and Uneyama T 2023 *Macromolecules* **56** 2217